JOURNAL OF OPTOELECTRONICS AND ADVANCED MATERIALS, Vol. 12, No. 7, July 2010, p. 1604 - 1618

Remote and local monitoring of dissolved and suspended fluorescent organic matter off the Svalbard

M. CISEK[a], F. COLAO[b], E. DEMETRIO[b], A. DI CICCO[b], V. DROZDOWSKA[a], L. FIORANI[b], I. GOSZCZKO[a], V. LAZIC[b], I. G. OKLADNIKOV[b], A. PALUCCI[b*], J. PIECHURA[a], C. POGGI[c], M. SIGHICELLI[b], W. WALCZOWSKI[a], P. WIECZOREK[a]

[a]*IO, PAN, Ul. Powstańców Warszawy 55, 81-712 Sopot, Poland*
[b]*FIM-FISLAS, ENEA, Via Enrico Fermi 45, 00044 Frascati, Italy*
[c]*BAS-IONIRP, ENEA, Via Enrico Fermi 45, 00044 Frascati, Italy*

Distribution maps of CDOM and algal pigments, both in superficial and deep waters, have been obtained operating a portable dual laser spectrofluorometer and a lidar fluorosensor equipments for the first time during two polish AREX oceanographic campaigns in 2006 and 2007 summertime in the Svalbard area. The different hydrological regimes strongly affected the biological factors in the waters around the Svalbard Islands as monitored during the campaigns with strong regional differentiations between the two years. The occurrence of large phytoplanktonic blooms and patches have been observed in the western area of the Spitsbergen Island coastline due to the nutrient release from pack ice and/or iceberg melting with values of more than 10 µg/l in both campaigns. Different CDOM fractions have been monitored with the remote and local instruments and inverse proportionality with salinity is confirmed along the water column. Phycobilin pigments, as phycoerythrin and phycocyanin accessory algal pigments, have been monitored in the northern area as well as tyrosine and tryptophan protein-like fluorescence distribution. The double filtration, performed with the dual laser spectrofluorometer, allows to retrieve the small fluorescence contribution due to NADPH and carotenoids pigments in the blue fluorescence emission. Successively, the large spectroscopic data base has been critically analyzed with a robust statistic instrument, thus identifying different marine provinces and retrieve distinctive CDOM fractions.

(Received January 22, 2010; accepted July 14, 2010)

Keywords: Laser fluorometry, Principal component analysis, Humic acid, Phytoplankton, Chlorophyll-a, Phycocyanin, Phycoerythrin, Arctic Ocean, Svalbard Islands

1. Introduction

The increased interest of international organizations on climate change strongly suggests to deeper investigate the role of oceanographic forcing on the global CO_2 sink, in particular in polar areas, where different seawater masses mixing and transformation processes generates the thermohaline circulation (Climate Change 2007). Among the different areas likely to be heavily affected by climate change, the Arctic Ocean shows a high potential risk due to observational evidences of decrease in snow and sea ice extent that will led to modifications in natural systems as well as in human activities. Circulation models supporting this hypothesis require long term experimental data in order to validate the physical and biological forecasts of the Arctic Ocean.

Nordic Seas (Norwegian, Greenland and Iceland Sea) are the transition zone between the Arctic Ocean and North Atlantic. Two branches of the Norwegian Atlantic Current (NwAC) carry warm, salty Atlantic Water (AW) northward through the Norwegian Sea (Orvik and Niiler 2002) (Fig. 1). The eastern branch, called the Norwegian Atlantic Slope Current (NwASC), flows over the Norwegian shelf break. The prolongation of this current continues northward over the Barents Sea slope and the west Spitsbergen shelf break, as the eastern branch (core) of the West Spitsbergen Current (WSC). The western WSC stream is a continuation of the NwAC offshore branch. It is an along-frontal baroclinic jet steered by the bottom topography of the Mohns and Knipovich Ridges (Piechura and Walczowski 1995). The western WSC branch is colder and less saline than the core. Due to the bottom topography, two WSC branches converge west of Spitsbergen at latitude 78° N and diverge again in the Fram Strait. The western branch mostly recirculates southward, the WSC core inflows into the Arctic Ocean through the eastern part of the Fram Strait, along the western Spitsbergen slope. Relatively warm (4 to 8 °C) and salty (34.9 to 35.3 PSU) Atlantic Water, carried by the NwAC and WSC, keeps Atlantic Domain of the Nordic Seas free of ice (Aagaard et al. 1987; Maslowski 1996; Piechura et al. 2001).

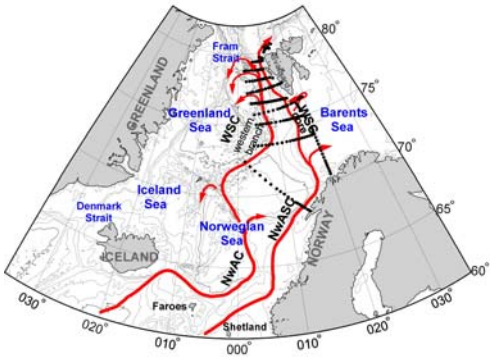

Fig. 1. Arctic main current system (Maslowski 1996). NwAC: Norwegian Atlantic Current, NwASC: Norwegian Atlantic Slope Current, WSC: West Spitsbergen Current.

To this respect, the Svalbard represent a border area between Atlantic and Arctic biogeographic zones, where the glacial input of freshwater and sediments create environmental gradients inducing large changes in community composition (Hop et al. 2002). Therefore, Svalbard can serve as an optimal Arctic research environment where it is possible to follow ecological changes, also because of the international polar research base of Ny-Ålesund.

Many terrestrial and marine components contain chromophoric chemical groups that emit fluorescence after proper excitation. Plant photosynthetic pigments (carotenoids and chlorophylls contained in chloroplasts), when excited with ultraviolet (UV) or visible light, show emission fluorescence in the visible or near infrared region, peculiar of the specific groups.

In natural waters, small idrosol components are present, mainly consisting of liquid or solid suspended particles. They are made by inorganic and organic matter that, in turn, can be disentangled in particulate organic matter (POM), i.e. phytoplankton, and dissolved organic matter (DOM).

Many of these components exhibit fluorescence emission upon UV excitation as aromatic amino acids bound to proteins (Determann et al.1998) (tryptophan and tyrosine) or phytoplanktonic pigments and chromophoric DOM (CDOM) (Coble et al. 1990).

Tryptophan and tyrosine are amino acids originated from proteins in DOM released by recent biological activity (fecal pellets), but also from phytoplankton (exudates) and bacteria. With the progress of degradation, living and non-living components contribute to size fraction of organic matter, determining different distribution of molecular mass fraction in seawater. Exudates and degradation products of the algae may lead to an increased signal in the protein-like fluorescence (Determann et al. 1998). The increased tyrosine- and tryptophan-like fluorescence, at an unchanged or lowered chlorophyll fluorescence level, may be indicative of bacterial biomass or "age of the bloom".

Algal pigments can be discriminated observing the signal at some assigned spectral bands (phycoerythrin and phycocyanin). Nevertheless, CDOM and algal photosynthetic components (i.e. NADPH and carotenoids) blue fluorescence could contribute to this signal (Steigenberger et al. 2004).

The Laser Applications Section (LAS) of the Italian National Agency for New Technologies, Energy and the Environment (ENEA) in Frascati, has developed different sensors for remote and in situ environmental monitoring along more than two decades of activities and one of its research branches is devoted to study the fluorescence of natural and pollutant components (R. Barbini et al. 1999; R. Barbini et al. 2003).

The experience gained in developing and operating a remote lidar fluorosensor (ELF) in different marine campaigns (Barbini et al. 1996a; Barbini et al. 1996b), either in European (Adriatic and Swedish Sea) and Polar (Southern Ocean and Antarctic Ross Sea) areas, was recently applied to realize a new portable laser fluorometer (CASPER) in the frame of a desertification project in Southern Italy (www.riade.net).

The peculiarities of this new instrument (portability, friendly use, double filtration, double excitation and flexible operation), employed in its first application in an inland water quality monitoring campaign, enable its exploitation also for marine applications.

In 2006, a collaboration started between LAS and the Institute of Oceanology (IO) of the Polish Academy of Sciences (PAS) in Sopot (www.iopan.gda.pl).The IO mission is to deeply investigate the marine environment, mainly in shelf seas and coastal regions, including the Baltic and European Arctic Seas, and in particular to carry out long term researches on the WSC (Walczowski and Piechura 2007). This last goal has been pursued since 1987 with the Arctic Experiment (AREX) oceanographic campaigns, now in the frame of the European project DAMOCLES (www.damocles-eu.org). LAS offered to IO its experience of extensive monitoring of CDOM and algal pigments during oceanographic campaigns in polar regions with two laser based instruments, i.e. the portable laser fluorometer and the remote lidar fluorosensor.

Distribution maps of CDOM and algal pigments, both in superficial and deep waters, have been obtained operating the two instruments in two AREX oceanographic campaigns (i.e. 2006 and 2007). The implementation of both instruments allowed to perform field studies on organic matter in large scale as the European Arctic. The remote and local fluorescence data have been discussed with respect to physical marine characteristics (temperature, salinity and density) and critically analyzed with a robust statistic instrument, thus identifying different marine provinces.

2. The polar cruise

IO monitors every summer the area of the Nordic Seas from the outermost Norwegian costs passing to the west side of the Svalbard Islands up to the 80° latitude north (Fig. 2) with the Research Vessel (R/V) Oceania. Several stations are located along the scheduled transects in order to deeply investigate changes in different marine behaviors. The exact repetition of the same stations every year allows a detailed investigation of the evolution of this Arctic area.

The R/V Oceania regularly performs two legs in the summer campaign. The first leg starts from the Tromsø harbour on the second decade of June. Then the ship sails towards the Svalbard Islands along the planned transects, shown in Fig. 2. At the beginning of July, the first leg ends in the Longyearbyen harbor. After logistic operations and turnover of scientific personnel, the second leg of the marine campaign starts. It ends with a second stop in Longyearbyen on the second decade of July. Eventually,

the ship goes back in Tromsø, at the beginning of August, ending the summer campaign.

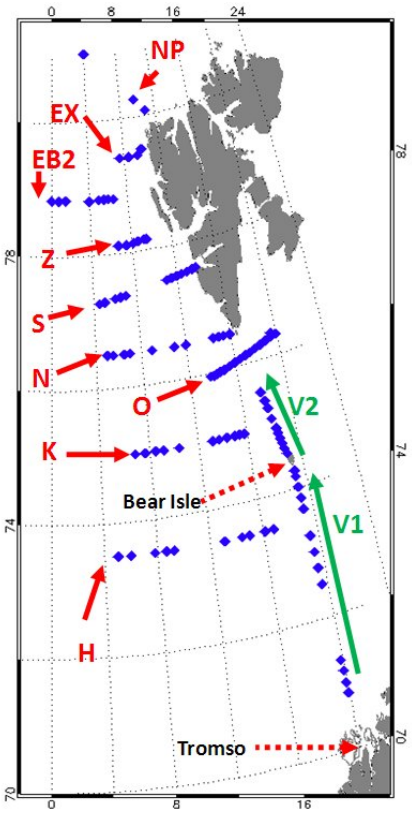

Fig. 2. Map of stations of the AREX 2006 and 2007 oceanographic campaigns with the indication of the different transects.

3. Instruments and methods

3.1 The portable laser fluorometer

The portable laser fluorometer CASPER is a general purpose instrument, patented after having been developed in our laboratory. The instrument makes use of the laser-induced fluorescence (LIF) technique to record spectra of the analyzed water samples. It is composed by two lasers emitting at 266 nm and 405 nm. The beams coming from the two sources, although following different paths, are combined in such a way that they are collinear at the exit optical plane. The laser beams illuminate the sampling chambers made by two quartz cuvettes. When the laser beam passes through the cuvette windows a laser induced fluorescence signal is emitted by the sample. The emitted light is collected and coupled by means of a fiber optic to an OceanOptics spectrometer for spectral analysis. Seawater is allowed to flow on a system of interconnected pipes until it completely fills each cuvette (Caputo-Rapti et al. 2008).

A proper characterization of seawater optical characteristics is accomplished by separating water constituents and allowing to enter in each cuvette only some of them. In particular, all seawater entering the laser fluorometer is filtered with a filter porosity of 30 µm, which let to pass phytoplankton of different size: microplankton (20-200 µm), nanoplankton (2-20 µm) and picoplankton (0.2-2 µm). The filtered water is allowed to enter the first cuvette C1 for determination of the pigment content: carotenoids, phycoerythrin, phycocyanin, chlorophyll-a (Chl-a). The outlet water from the first cuvette passes a combination of two filters (a first filter of 0.8 µm porosity, to remove biggest algal cells, and a second filter of 0.22 µm porosity, to remove all the other particles) and finally fills the cuvette C2 for determination of dissolved substances (CDOM, tryptophan, tyrosine). The parameters used in the fluorometric operations are specified in Table 1.

Table 1. Operating parameters of the portable laser fluorometer CASPER.

Cuvette	Filter	Function
C1	30 µm	Algal pigment detection (phycoerythrin, phycocyanin, Chl-a)
C2	0.22 µm	DOM detection (CDOM, tryptophan, tyrosine)

Flush cycle	100 ml seawater + 100 ml fresh drinking water
Load cycle	100 ml seawater

CASPER has been operated for the first time for seawater monitoring in both AREX 2006 and 2007 oceanographic campaigns, hosted inside a wet laboratory of the R/V Oceania. In both campaigns, the protocol adopted for CASPER operation foresees the water spilling from the Niskin bottles of the rosette at different depths along the scheduled station. Calibration and measurement procedures of the instrument implemented during the marine campaigns follows the already published protocol are reported in the literature (Caputo-Rapti et al. 2008). The measurement procedure implemented that includes a control of the linear responsivity of the apparatus, with samples of Milli-Q water, and the calibration with standard solutions provided by Sigma-Aldrich.

The data analysis procedure includes a list of actions to be followed before the final data release, summarized as follows:

- Subtraction of the electronic and light backgrounds from the fluorescence spectrum.
- Lorentzian fit of the peaks of the spectrum.
- Calculation of the integral of the spectrum at some preselected bands, corresponding to the emission of the relevant substances (e.g. centered

at 680 nm for Chl-a) within a fixed bandwidth (usually 10 nm).

- Subtraction of the spectral background from the integral at the preselected bands (e.g. subtraction of the tail of the CDOM peak from the Chl-a band).
- Preliminary release of the substance concentrations in Raman unit (RU), i.e. rationing the integral at the preselected bands to the integral of the Raman peak.
- Final release of substance concentrations in absolute units (e.g. mg m^{-3}) by calibration with standard solutions.

Time, latitude, longitude and depth of the sampled site were stored together with spectroscopic information for a further elaboration. The spectral bands employed in the data analysis are given in Table 2 are given.

Table 2. Peak position of spectral bands in the LIF signal. λ_{exc} is the excitation wavelength, λ_{em} is the emitted wavelength.

Component	λ_{exc} [nm]	λ_{em} [nm]
Water (Raman scattering)	266	292
Tyrosine	266	315
Tryptophan	266	350
Hydrocarbons	266	420
CDOM	266	450
Water (Raman scattering)	405	470
Phycoerythrin	405	580
Phycocyanin	405	630
Chl-a	405	680

In case of occurrence in seawaters of intense algal bloom (Chl-a concentration > 1 µg/l), the blue fluorescence emission, mainly ascribed to CDOM content, can also contain contributions due to spectral absorption and re-emissions from xanthophyll, fucoxantin (Shreve et al. 1991) and minor light harvesting carotenoids (Mimuro et al. 1993). Even if the last contribution is very small (Palucci 2006), this effect will overlap the CDOM fluorescence as a Gaussian term peaked at 490 nm. In Fig. 3 the fluorescence emission of the same water sample before (Fig. 3a) and after (Fig. 3b) the second filtration stage is compared. In the second spectrum (Fig. 3b), the decrease in the blue emission fluorescence is of the order of 20%. Therefore, we will consider the carotenoids contribution, as the difference between the amplitude of the Gaussian term peaked at 490 nm before and after the second filtration stage. It is expressed in RU by dividing its spectral intensity by the Raman signal. This choice is validated by the correlation analysis where a good agreement is observed between Chl-a and carotenoids.

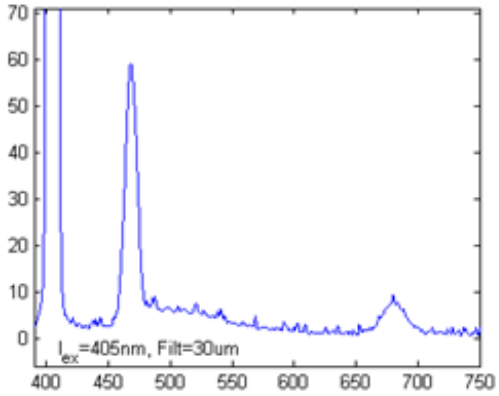

a

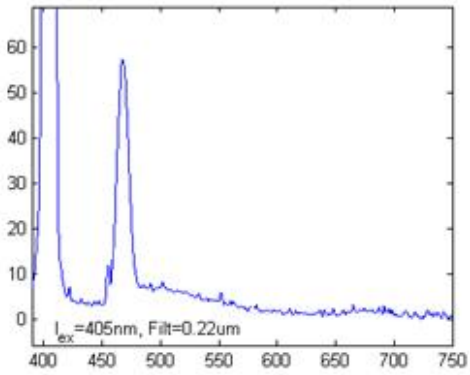

b

Fig. 3. Fluorescence emission of the V16 sample collected at the sea surface: a) after 30 µm filtration; b) after 0.22 µm filtration (the Chl-a concentration was 1.4 µg/l).

3.2 The remote lidar fluorosensor

The remote lidar fluorosensor ELF allows the continuous and automatic remote monitoring of LIF emitted by surface seawater layers (up to 30 m) along the cruise. Details on the lidar system, the ancillary instruments, e.g. solar radiometer and global positioning system (GPS), and data analysis are given in the literature (Barbini et al. 1999).

Like CASPER, ELF is based on LIF: CDOM, phycoerythrin, phycocyanin and Chl-a are detected measuring their emission at 450, 580, 650 and 680 nm, respectively, after excitation by a frequency-tripled Nd:YAG laser at 355 nm. The Raman signal is measured at 404 nm and the background is evaluated at 430 and 630 nm. Thanks to narrowband filtering and electronic gating, LIF signals do not need corrections for the spectral

characteristics of solar irradiance and surface reflectance. Furthermore, due to the short distance from the target, atmospheric effects are negligible. This explains why ELF data can be regarded as sea truth and have been used for the calibration of the bio-optical algorithms of the ocean color satellite radiometers MERIS, MODIS and SeaWiFS that determine the Chl-a concentration from the blue-to-green ratio of the sunlight backscattered by the sea surface (Fiorani et al. 2008).

The data coming from the different ELF detection channels and the ancillary information (Barbini et al. 2001) are simultaneously stored and successively. ELF is calibrated with the simultaneous measurements of CASPER in the same seawater.

4. Results

The operation of the portable laser fluorometer CASPER and the remote lidar fluorosensor ELF during AREX 2006 and 2007 allowed to retrieve a large dataset of fluorometric measurements over a large European arctic area and the results released as depth distributions along the transects and superficial thematic maps of the investigated area.

In particular, CASPER was employed in two legs of AREX 2006 and CASPER and ELF were simultaneously operated in the second leg of AREX 2007. Table 3 are lists the transects of both campaigns and the number of stations and samples analyzed with CASPER. ELF measurements are not tabled due to the continuous operation mode of the instrument.

As indicated in Table 3, more than 300 samples at different depths along the scheduled stations were analyzed by CASPER only in the AREX 2006 campaign. The complete dataset has been grouped in three main depth layers as superficial (from 0 m to 20 m; about 100 samples), euphotic (from 0 m to 100 m; about 150 samples) and aphotic (from 100 m to bottom; about 140 samples). The euphotic zone is the upper illuminated zone of aquatic ecosystems. It is above the compensation level and therefore it is the zone of effective photosynthesis. In marine ecosystems it is much thinner than the deeper aphotic zone (below the level of effective light penetration): the euphotic zone typically reaches 30 m in coastal waters but can extend up to 100 m in open ocean waters.

Table 3. List of transects stations and samples of AREX 2006 and 2007.

	2006			2007		
Transect	Stations	Samples	Period	Stations	Samples	Period
V	15	32	20-23/06/06	5	10	08-09/07/07
H	8	29	24-27/06/06			
K	11	52	28-29/06/06	4	12	10/07/07
V2	11	23	30/06/06			
O	16	50	01-02/07/06	5	18	07-08/07/07
N	13	48	06-08/07/06	4	22	11-14/07/07
S	12	38	09-10/07/06			
Z	7	23	12/07/06	8	34	14-16/07/07
EB2	3	12	12/07/06	9	34	16-18/07/07
NP	4	12	15-16/07/06			
EX	3	9	17/07/06	7	10	21-22/07/07
Total	103	328	28 days	42	140	16 days

The scenario monitored with CASPER during 2006, for different fluorescent components, is illustrated in Fig. 4. The superficial distribution has been selected, due to close similarities with the euphotic zone as far as the occurrence of algal pigment is concerned.

In the same figure, the temperature behavior is reported for completeness of information and comparison purposes.

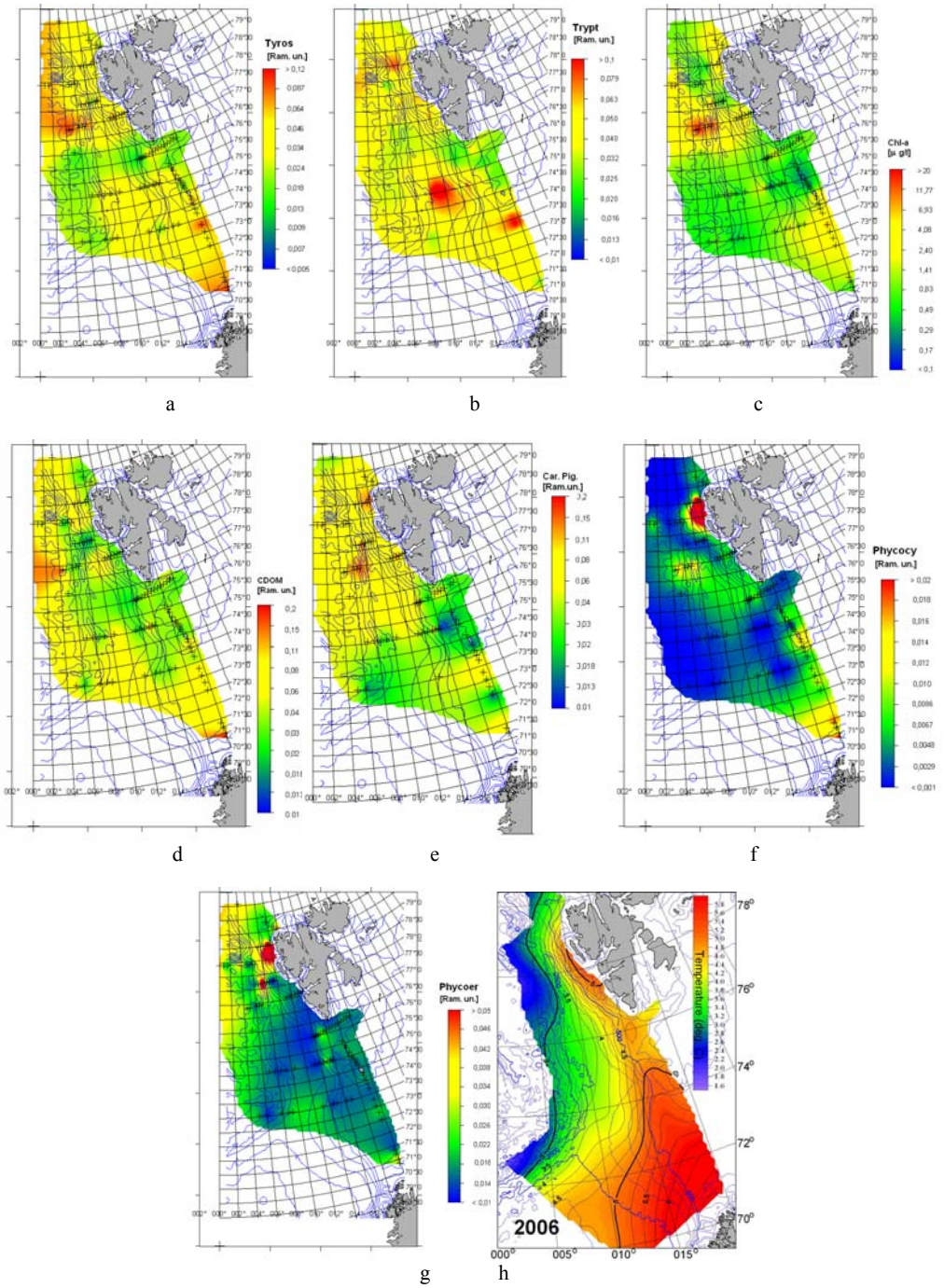

Fig. 4. Superficial distribution measured by CASPER during AREX 2006 of: a) tyrosine [RU]; b) tryptophan [RU]; c) Chl-a [µg/l]; d) CDOM [RU]; e) carotenoids [RU]; f) phycocyanin [RU]; g) phycoerythrin [RU]; h) temperature (°C). The black crosses are the stations.

CASPER measurements, collected along the water column at different stations, allowed also to obtain a detailed deep split into the transects.

An example of dissolved and particulate matter depth distribution is reported in Fig. 5. Also in this case, the corresponding temperature is reported for the sake of comparison.

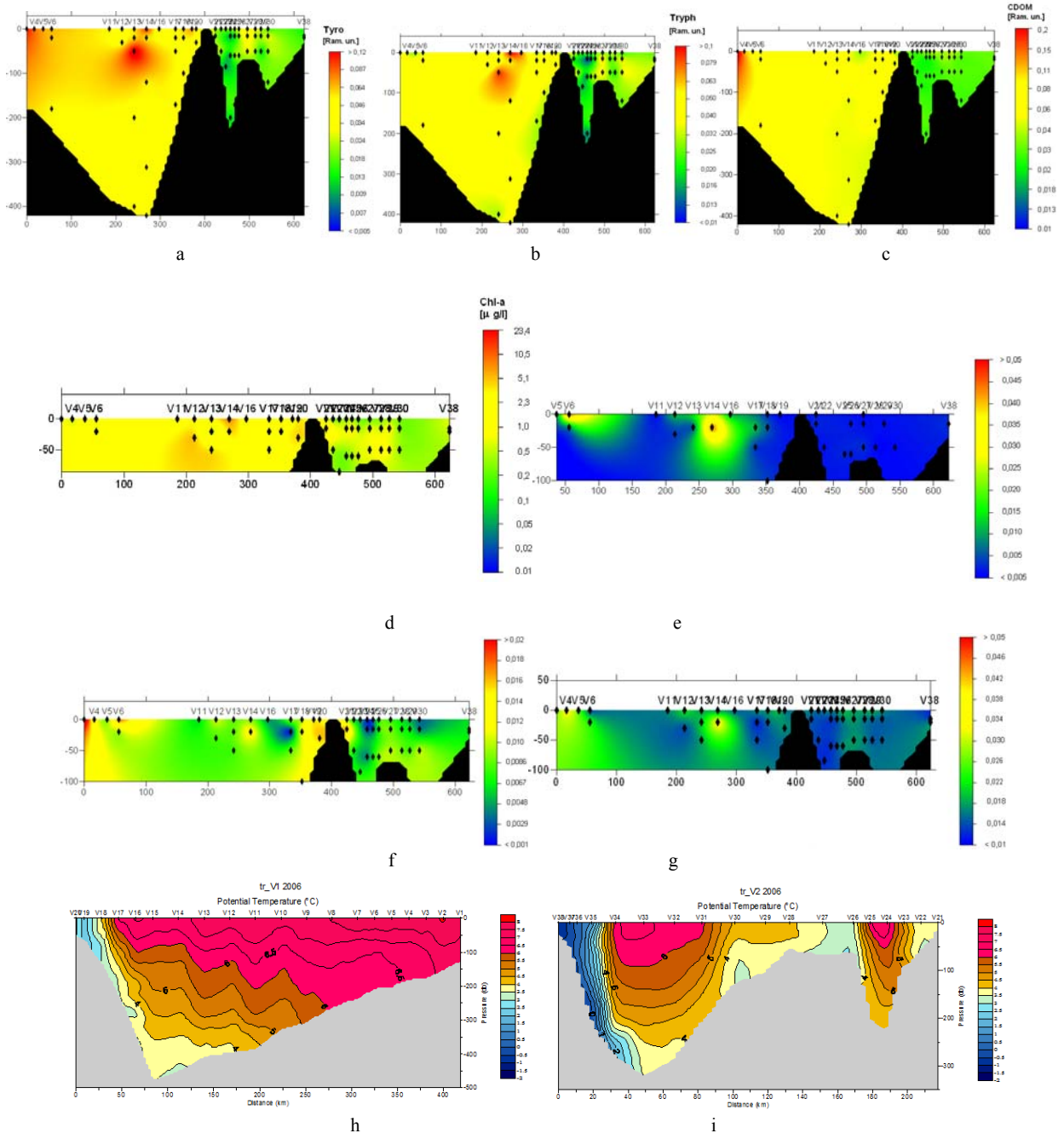

Fig. 5. Vertical distribution measured by CASPER during AREX 2006 of: a) tyrosine [RU]; b) tryptophan [RU]; c) CDOM [RU]; d) Chl-a [µg/l]; e) carotenoids [RU]; f) phycocyanin [RU]; g) phycoerythrin [RU]; h) temperature (°C) in the first leg of transect V (from Tromsø to the Bear Island); i) temperature (°C) in the second leg of transect V (from the Bear Island to the southern coast of Spitsbergen Island). The black diamonds are the measurement points.

ELF was employed during the second leg of AREX 2007. It operated continuously H24 and sounded remotely the surface layer, thus providing a spatiotemporal picture of DOM and algal pigments in a wide oceanic region. The lidar system performs a monitoring of the investigated marine environment without sample manipulation.

The thematic maps of CDOM, phycoerythrin, phycocyanin and Chl-a measured by ELF during the oceanographic campaign are shown in Fig. 6, together with the superficial temperature distribution map.

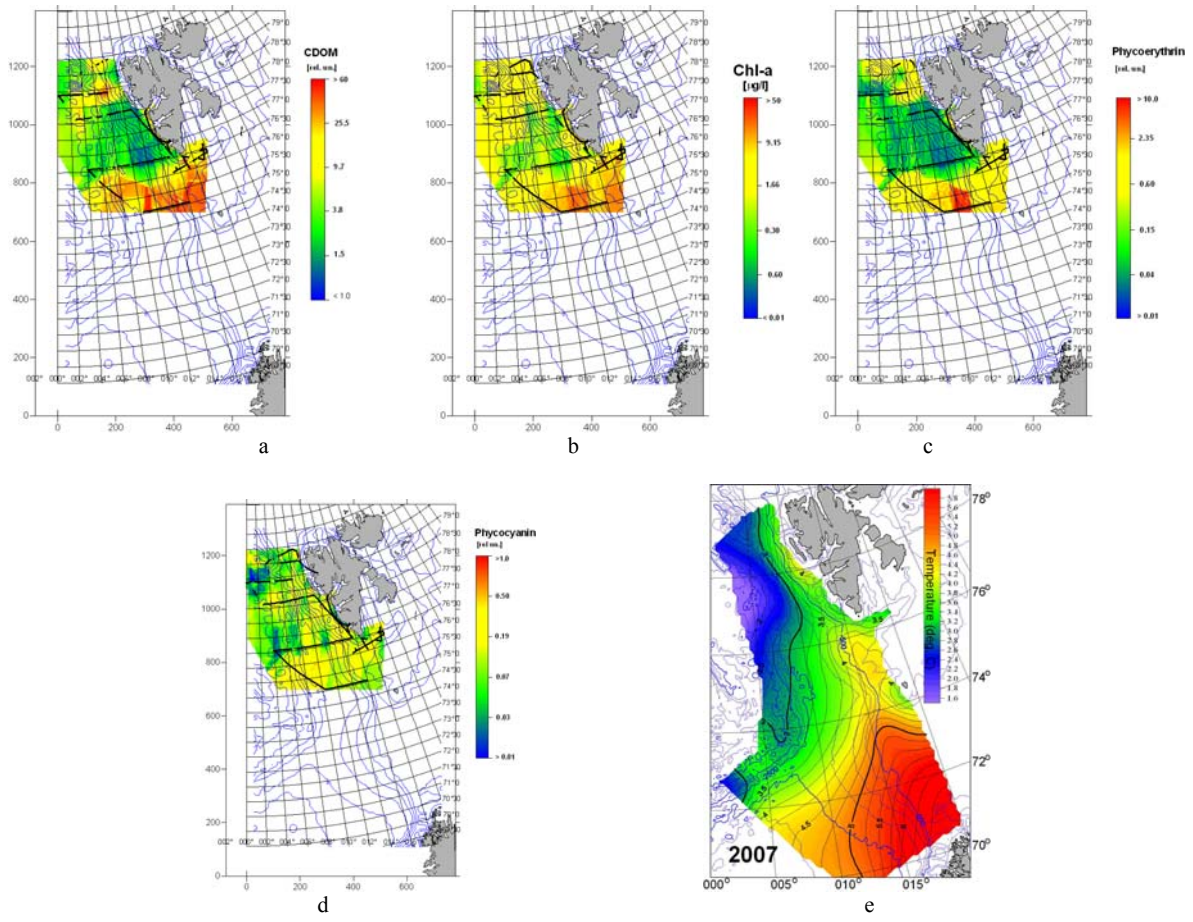

Fig. 6. Superficial distribution measured by ELF during AREX 2007 of: a) CDOM [RU]; b) Chl-a [µg/l]; c) phycoerythrin [RU]; d) phycocyanin [RU]; e) temperature (°C). The black line is the ship track..

5. Discussion

The waters around the Svalbard Islands are exposed to different hydrological regimes and biological factors, as well as the sea ice conditions, already described in the introduction. Therefore, phytoplankton biomass and composition in these polar regions vary considerably, showing a spatial heterogeneity of plankton communities (Owrid et al. 2000).

The biomass distribution in both campaigns shows the occurrence of large phytoplanktonic blooms and patches in the western area of the Spitsbergen Island coastline where the release of nutrient from pack ice and/or iceberg melting strongly contribute to fertilize this area (Fig. 4c and Fig. 6b) (Inall et al. 1992). Values of more than 10 µg/l were monitored in both campaigns, thus supporting the hypothesis that the Svalbard Islands marine ecosystem is a high productive environment.

As a general trend, in 2006 the release of CDOM and high phytoplankton concentration are strongly correlated (Fig. 4d and Fig. 6a), as confirmed by the plot of their values averaged along the latitude (Fig. 7). Moreover, Chl-a is anticorrelated with temperature, showing that colder waters are more productive.

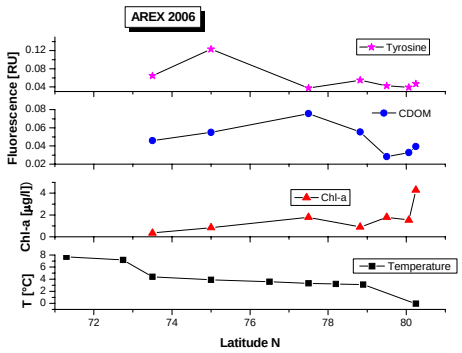

Fig. 7. Averaged determination of physical and biological parameters along the latitude; a) Temperature [°C]; b) Chl-a [µg/l]; c) CDOM [RU]; d) Tyrosine [RU].

Among the different effects that can act in changes of CDOM content (terrestrial or glacial run-off, precipitation, evaporation, biological interaction, photooxidation), salinity is linked to the water mixing processes (Clark et al. 2004).

The overall behavior of CDOM fluorescence emission, as monitored in the Arctic waters, is plotted versus the salinity in Fig. 8: the inverse proportionality between CDOM and salinity that characterizes other oceanic provinces, has not been observed everywhere, thus confirming the irregularity and dynamicity of the polar environment, where diverse marine currents and water masses are present (see Table 4). This unclear behavior, in our measurements, is due to the lack of information in deeper waters, because we concentrated our efforts in analyzing with the portable fluorometer in more detail the Euphotic zone and compare the data with the corresponding lidar data. Nevertheless, some similarities, with other oceanic waters, have been observed.

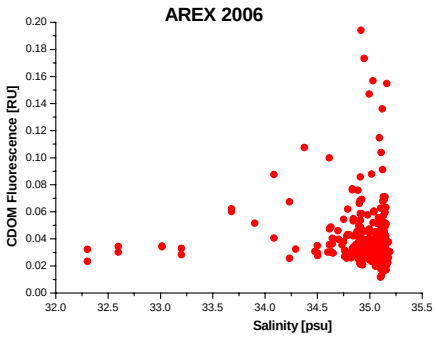

Fig. 8. Scatter plot of CDOM fluorescence versus Salinity for all the measurements of AREX 2006.

Table 4. Fram Strait water masses characteristics (Schlichtholz and Houssais 1999).

Item	Acronym [a]	Temperature	Salinity [psu]
1	PW	θ < 0ºC θ > 0ºC	S < 34.7 S < 34.4
2	AWw	θ > 2ºC	S > 34.91
3	AWf	θ > 1ºC	34.4 < S < 34.91
4	AWc	0ºC < θ < 2ºC	S > 34.91
5	MAW	0ºC < θ < 1ºC	34.4 < S < 34.91
6	AIW	- 1.1ºC < θ < - 0.5ºC - 0.8 ºC < θ < 0ºC	34.7 < S < 34.9 34.9 < S < 34.92 [b]
7	UPDW	- 0.5 ºC < θ < - 0ºC	34.7 < S < 34.9 [c]
8	NSDWw	- 0.8 ºC < θ < - 0.5ºC - 0.5 ºC < θ < 0ºC	34.9 < S < 34.92 [d] 34.9 < S < 34.92 [e]
9	CBDW	- 0.8 ºC < θ < - 0.5ºC	S > 34.92
10	NSDWc	- 1.1 ºC < θ < - 0.8ºC	34.9 < S < 34.92
11	EBDW	- 1.1 ºC < θ < - 0.8ºC	S > 34.92
12	GSDW	θ > - 1.1ºC	34.7 < S < 34.92

[a] PW - Polar Water; AWw - warm Atlantic Water; AWF - fresh Atlantic Water; AWc - cold Atlantic Water; MAW - Modified Atlantic Water; AIW - Arctic Intermediate Water; UPDW - Upper Polar Deep Water; NSDWw - warm Norwegian Sea Deep Water; CBDW - Canadian Basin Deep Water; NSDWc- cold Norwegian Sea Deep Water; GSDW - Greenland Sea Deep Water; EBDW - Eurasian Basin Deep Water.

[b] if a salinity minimum is found in the range - 1.1ºC< θ < - 0.5ºC; 34.7 < S < 34.9.

[c] only if the mean h}*S* regression slope is negative.

[d] if not AIW.

[e] if not AIW nor UPDW

In fact, the anticorrelation behavior is observed along the water column in selected stations, where from the batimetry analysis, allows for the occurrence of superficial, intermediate and deep waters, respect to the stations, reported in Fig. 10, related only to superficial waters.

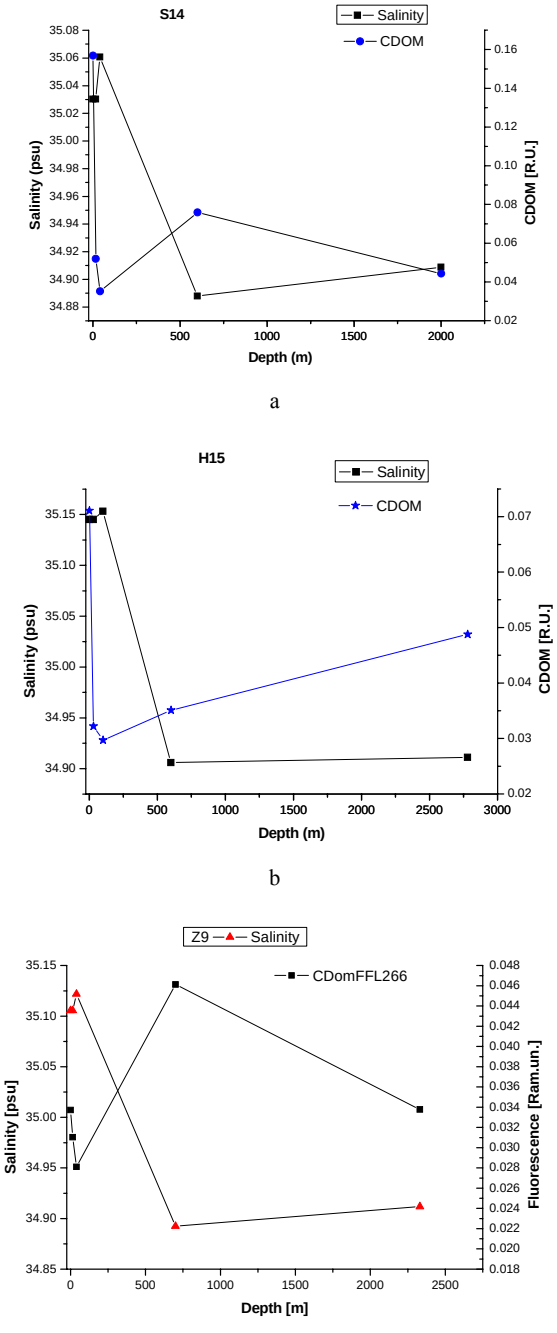

Fig. 9. Salinity and CDOM as a function of depth in different stations: a) S14; b) H15 and c) Z9.

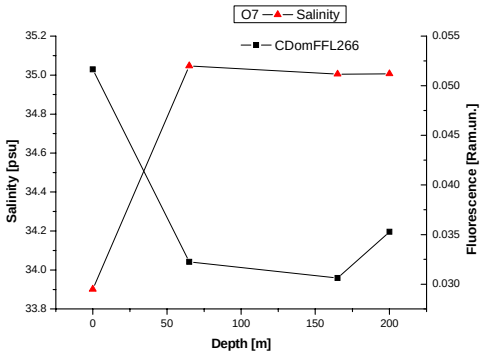

a

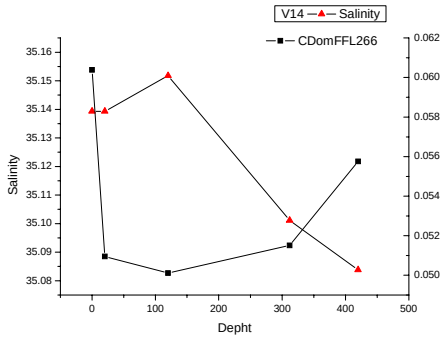

b

Fig. 10. Salinity and CDOM as a function of depth in the O7 (left) and V14 (right) stations.

Phycobilin pigments, as phycoerythrin and phycocyanin accessory algal pigments, have been observed in the northern area (Fig. 4f and Fig. 4g, respectively), close to the northern Spitsbergen coastline, during AREX 2006 and in the southern area (Fig. 6c and Fig. 6d), during AREX 2007. The occurrence of these fluorescent pigment is the indication of Cryptophyceae Cyanophyceae and Rhodophyceae algae in the natural phytoplanktonic community.

Tyrosine and Tryptophan protein-like fluorescence distribution is depicted in Fig. 4a and Fig. 4b, respectively, for AREX 2006. The effect of a strong biological activity in superficial waters is clearly evident from the maps, with a strong correlation between tyrosine and biomass production (Fig. 4c). The occurrence of maxima below the photic zone can be ascribed to an evidence of bacterial decomposition of DOM.

The contribution due to NADPH and carotenoids pigments has been reported in the superficial distribution map of Fig. 4e. These components are recognized as chemotaxonomic biomarkers of the phytoplanktonic biomass distribution, but their different spatial distribution is due to changes in radiance and seawater currents (Steigenberger et al. 2004). The map of Fig. 4e, in comparison with biomass distribution (Fig. 4c), shows overlapping areas in the central and northern seawaters of the Spitsbergen region, but a different behavior in the southern Atlantic section, thus supporting the hypothesis of a different primary productivity of the investigated environments.

Statistical analysis of the CASPER dataset

Principal component analysis (PCA) (Jolliffe 2002) has been applied on the overall dataset collected by CASPER during AREX 2006 on the stations listed in Table 3. PCA can actually be used as a way to better analyze large amount of data, especially in those situations where a strong correlation among measurements on the samples is expected. Actually, it is necessary to address at least the following fundamental problems, namely:

- how many spectral bands are needed to completely describe each spectrum collected by CASPER?
- is there any possible way to classify different waters (coastal, oligotrophic oceanic, deep and surface waters, etc.) by means of an automated procedure?
- can the acquisition be simplified in order to use data correlation (and/or data redundancy) to reduce the number of acquired spectra?

PCA can answer such questions, especially the first one. To investigate these aspects, PCA has been applied to the entire dataset. Different ways to reduce the spectral resolution have been tried (binning at 5, 10, 25, 50 and 100 nm) and the optimal compromise was reached for bins of 25 nm.

Complete AREX 2006 dataset

The PCA results from a run on data binned at 25 nm are reported in Fig. 11, where the coefficients of the first four principal components are plotted versus the emission wavelength. To distinguish among coarse and fine filtrations different suffixes have been used: F stands for single filtration at 30 µm and FF stands for double filtration at 30 and 0.22 µm. Similarly, the laser excitation wavelengths have been indicated by means of the suffix UV and VS, meaning 266 and 405 nm, respectively.

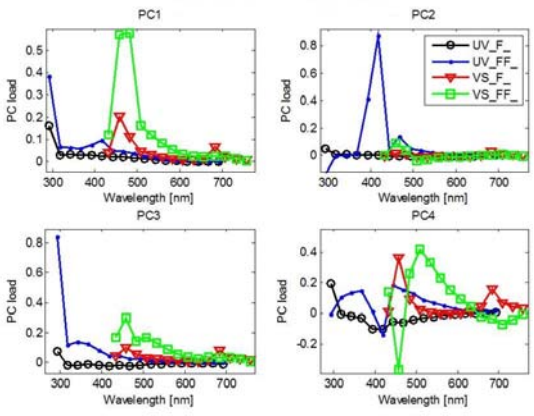

Fig. 11. Coefficients of the first four principal components for all the data of AREX 2006.

It may be noted that the spectral coefficients of the first principal component (PC1) closely resemble a spectrum obtained by a simple average of the spectra contained in the entire data set. Since PC1 is able to explain a noticeable amount of the variance (more than 60%), as shown in Fig. 12, we may conclude that the total signal output from the spectrometer roughly indicates the water type. It is to be expected that oligotrophic waters are associated with relatively high Raman signal and low fluorescence from CDOM excited at 405 nm and CDOM excited at 266 nm. The contribution from UV_F water sample spectra appears of little significance.

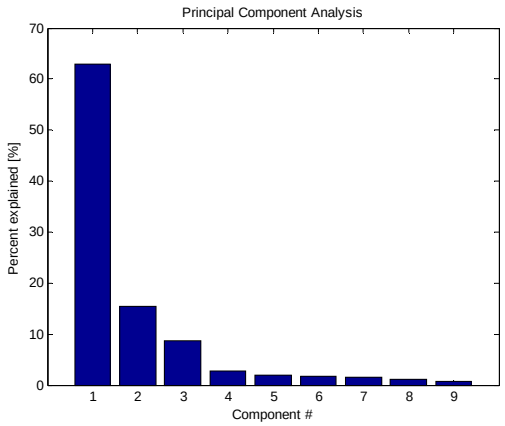

Fig. 12. Percent of variance explained by the principal components. Only the first 9 components are shown.

The second component (PC2) is characterized by a relatively intense peak attributed to CDOM emission at 415 nm. Indeed it contributes differently in singly and doubly filtered water, as illustrated for example by the 400 nm component of doubly filtered water dominating the contributions to PC2. As noted also for PC1 the contribution from UV_F appears of little significance.

The third principal component (PC3) is dominated by the Raman emissions at around 290 and 450 nm and the contribution from the Chl-a fluorescence at 680 nm starts to gain importance. Although PC3 accounts for less than 10% of the overall spectra variance (Fig. 12), it has an important meaning from the point of view of water classification, because it contains the contribution from algae, a relevant water constituent, and then it is expected it will play a significant role for the water type discrimination.

The last contribution taken into account at the present moment, concerns the fourth principal component (PC4) that gives a contribution to the variance of approximately 5%, as shown in Fig. 12. It appears dominated by an approximately equal contribution from CDOM excited at 405 nm and Chl-a with respect to the Raman emission. The relevance of PC4 is related to its expected capability to discriminate turbid water (low Raman signal and high fluorescence from CDOM excited at 405 nm) with respect to eutrophic water (high fluorescence from CDOM excited at 405 nm and Chl-a), thus complementing the picture given by the previous components.

Based on the observation that, starting with the fifth principal component, the explained variance is less than 3%, it has been decided to disregard the principal components beyond PC4, because they play a minor role in the assessment of water type.

Concluding this preliminary section, we can partially answer the third question raised earlier, i.e. that on data redundancy, by noticing that the contribute of UV_F spectra are effectively of little significance in all the principal components and can therefore be ignored.

Once the PCA coefficients are obtained they can be used to compute the so called scores, corresponding to the original data mapped into the new coordinate system defined by the principal components. There are so many data points as it is the number of samples (one per each depth in every station). Scores are represented in two dimensional plots reporting the ratings data, projected onto two consecutive principal components (note that the scores computed by PCA have zero mean).

Fig. 13 shows PC2 versus PC1 and PC4 versus PC3 for the complete data set. In order to allow sample recognition and possibly to distinguish among different water types, data are represented by symbols and colors uniquely identifying the transects. Several interesting aspects appear from the observation of Fig. 13, namely:

- PC1 and PC2 anticorrelate;
- the points corresponding to the same transect tend to form clusters.

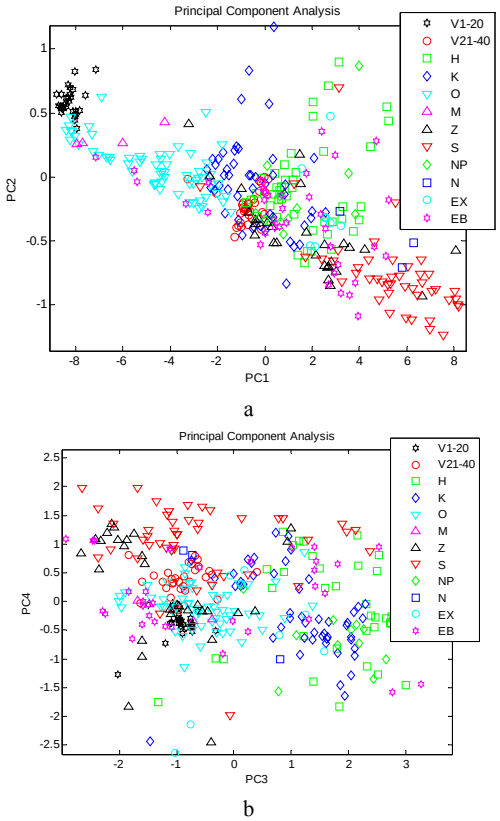

Fig. 13. Score plots of PCA for all the data of AREX 2006: a) PC2 versus PC1, and b) PC4 versus PC3.

The anticorrelation of PC1 and PC2 could induce to look suspiciously at the processed data, because PCA transforms the input data set, described in terms of its original components, in a new data set in which correlation has been removed. Since points tend to occur apart from the line individuated by the bottom of the cluster towards higher values of PC2, the ensemble average can still have a numerically zero correlation, in spite of the fact that cluster centers arrange approximately along a straight line. According to the above interpretation (PC1 and PC2 correspond roughly to Raman and CDOM signals, respectively), this result shows that an increase of the total LIF signal (PC1) corresponds to a decrease in the principal components dominated by fluorescence from CDOM excited at 405 nm and CDOM excited at 266 nm (PC2), thus giving the base for establishing a negative correlation between water transparency and dissolved matter content. To reinforce this observation let us take into account data as much homogeneous as possible, i.e. restricting the comparison just to data collected during the same oceanographic leg: we observe that water sampled at increasing latitudes is characterized by an increase in the component PC2, i.e. by an increase of the CDOM content. Indeed, with the only exception of the transect V1-20, the cluster centers of the transects from H towards K and then O and V21-40 show an increase in PC2 and similarly do the transects from S towards Z and then EX and EB. Although these results agree with similar observations made in the past (Colao et al. 2008), it has to be kept in mind that the total signal intensity is linearly and strongly coupled to the optical power of the excitation source. Unfortunately, since the system was not equipped to measure that optical power, the observed trend has to be considered only qualitatively.

As far as the clustering of data corresponding to the same transect is concerned, it should be noticed that what has been observed in Fig. 13a is confirmed in Fig. 13b. Although the plot of PC4 versus PC3 appears much more scattered than the plot of PC2 versus PC1, the clusters corresponding to different transects can be easily distinguished. This clustering effect can be explained by the smooth and persistent change of the optical characteristic of water sensed by CASPER going from coastal to oceanic areas and then back to coasts. To pursue further on this analysis it is needed to introduce additional considerations and to treat the water samples separately in relation to their sampling depths.

Superficial waters dataset

The superficial waters dataset takes into account only seawater sampled at depths not below 100 m. Since this depth limit was selected to retain only samples belonging to the photic layer, it is expected that they form a homogeneous dataset that has been processed exactly as described in the preceding section.

Fig. 14 shows the coefficients of the first four principal components versus the emission wavelength. Symbols and colors are the same of Fig. 11.

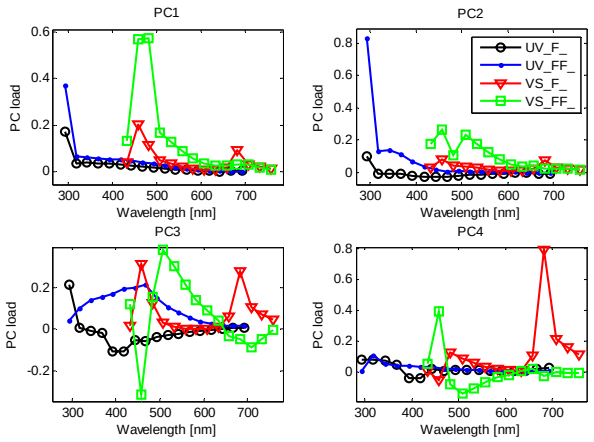

Fig. 14. Coefficients of the first four principal components for the superficial waters (not below 100 m) of AREX 2006.

At a first glance, Fig. 11 and *Fig. 14*Fig. 14 make evident that superficial waters are characterized by different coefficients, thus indicating that spectrum interpretation has to be carried out considering carefully specific peculiarities of the water sample. A more careful inspection of these figures reveals some interesting similarities and differences. The coefficient of PC1 represents again an average spectrum, although this time it is relative only to superficial waters. The coefficient of PC2 is no more dominated by the 400 nm peak due to CDOM in the UV_FF spectrum, while it shows contributions from Raman and protein-like fluorescence.

Indeed the disappearance of the 400 nm band suggests that different principal components are significant for superficial water spectra. A possible explanation is that hydrosols dispersed in superficial waters give the greatest contribution to fluorescence at 450 nm and have a grain size blocked by the 30 μm filter, thus they might be associated with both living and senescent algal cells. Moreover, the UV_FF significant contribution to PC2 in the protein-like spectral region can be correlated with the presence of a rich biological life, especially when the walls of died cells is broken, allowing their content to be released and float in water. Also the reduced importance observed in the spectra relative to 30 μm filtered water is well documented by UV_F spectra popping up only in PC5 (not shown), while their contribution was negligible in the previous principal components. Finally, we note that PC2 and PC3 of Fig. 14 are similar to PC3 and PC4 of Fig. 11 and thus comments on PC2 and PC3 of Fig. 14 are similar to those made for PC3 and PC4 of Fig. 11.

Fig. 15 shows the plot of the second component versus the first one for the superficial sample dataset with the same symbols and colors used in Fig. 13. It can be noticed that:

- the first and the second components are no more anticorrelated;
- data points corresponding to the same transect tend to form clusters.

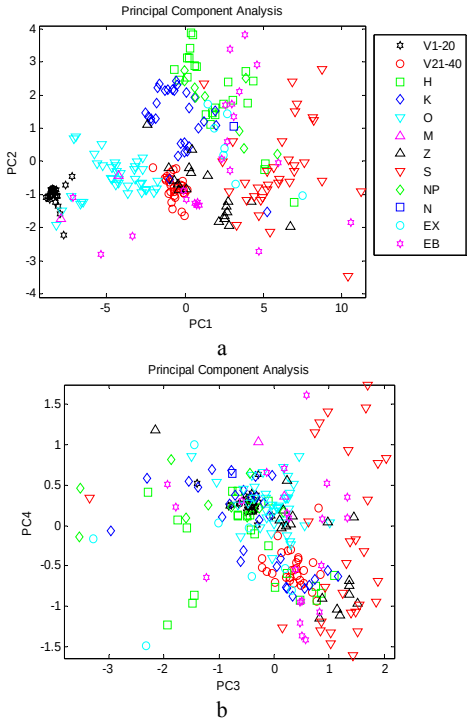

Fig. 15. Score plot of PCA for the superficial waters (not below 100 m) of AREX 2006: a) PC2 versus PC1, and b) PC4 versus PC3.

Since no evident anticorrelation has been observed, it can be concluded that superficial waters are much more mixed than deep waters. Data belonging to different transects tend to form clusters better defined than before, thus indicating that the regional characteristics can be used to discriminate water masses. In general, it can be noticed that coastal and offshore waters are almost uniformly scattered along the PC1 axis and that oceanic waters tend to have high values of PC2, a principal component dominated by protein-like substances. On the other hand, Fig. 15b shows more scattered data with coastal water samples concentrated significantly on high values of PC3. A possible explanation of this behavior is that coastal waters are characterized by an increase of both Chl-a and CDOM which have approximately the same weight in PC3.

Deep waters dataset

The deep waters dataset takes into account only seawater sampled at depths below 100 m. Since this depth limit was selected with the purpose of excluding samples belonging to the photic layer, it is expected that this dataset is dominated only by aphotic waters. The deep waters dataset has been processed exactly as the other ones.

Fig. *16* shows the coefficients for the first four principal components versus the emission wavelength; the symbols and colors are the same used in Fig. 11.

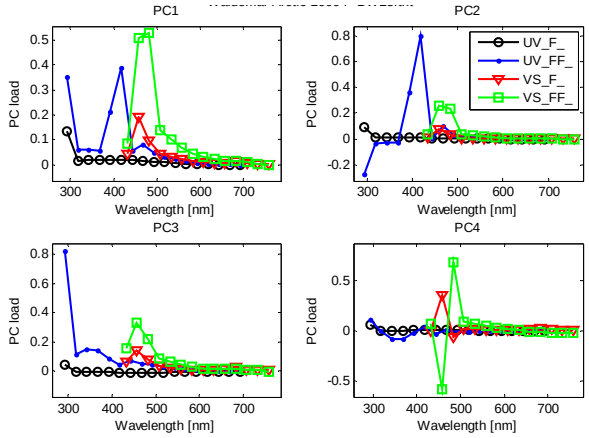

Fig. 16. Coefficients of the first four principal components for the deep waters (below 100 m) of AREX 2006.

Fig. *16* reveals that the principal components of the deep waters have coefficients quite similar to those obtained for waters of all depths (Fig. 11). Minor but not negligible differences can be noticed in PC4, where – as it can be expected in the aphotic layer – the contribution on the spectrum given by the Chl-a fluorescence at 680 nm has now almost completely disappeared (the very small bump around that wavelength is due to a possible slight contamination with water sampled at shallow depths). For the deep waters dataset, PC1 is able to explain about 52% of the variance, which is essentially the same contribution observed in the previous cases.

Fig. 17 shows the plot of the second component versus the first one for the superficial sample dataset with the same symbols and colors used in Fig. 13. It can be noticed that:

- the anticorrelation already noticed in Fig. 13a is now much more evident;
- data points corresponding to the same transect tend to form clusters;
- data scattering is strongly reduced because the points that tend to occur apart from the line individuated by the bottom of the cluster towards higher values of PC2 have now disappeared.

As far as the interpretation of the plot of PC2 versus PC1 is concerned, it is possible to repeat the discussion made in the section dealing with water samples from all depths, although the trend can now be appreciated more easily. With the exception of the transect V21-V40, it can be observed a increase of PC1 and a decrease of PC2 while samples go toward clearer waters.

In Fig. 17b, it can be observed that the samples belonging to the same transect form clusters more defined with respect to those of Fig. 11b and Fig. 15b. This behavior can be explained by the more homogeneous

water samples, less influenced by remnants due to biological life.

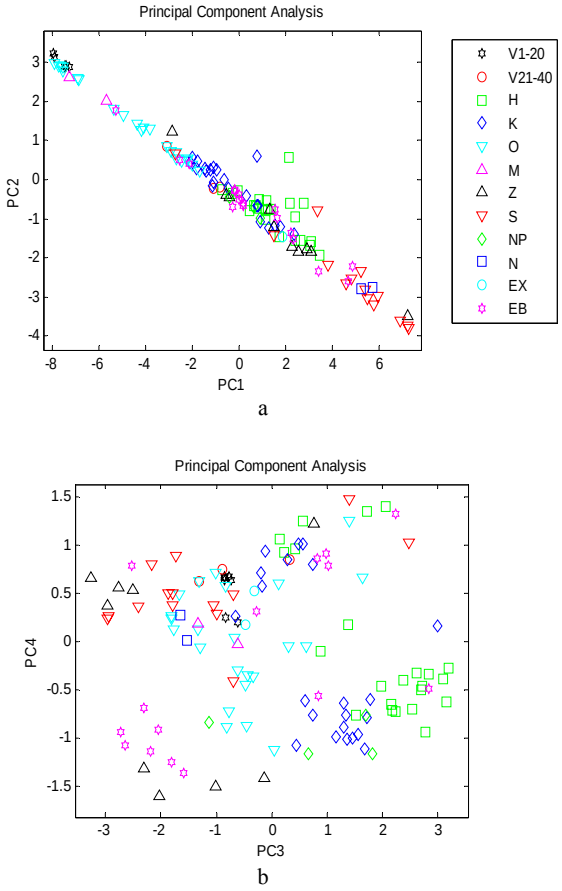

Fig. 17. Score plot of PCA for the deep waters (below 100 m) of AREX 2006: a) PC2 versus PC1, and b) PC4 versus PC3.

6. Conclusions

The collaboration between IO and LAS during AREX 2006 and 2007 resulted in an increased understanding of Arctic seawaters and in a technological improvement in laser systems that have been operated continuously in a large scale thus allowing to deeply investigate the different fluorescence fractions. This the first attempt to combine remote and local fluorescent data.

The monitored area is characterized by important seasonal variations linked to the heavy impact of nutrient availability, water temperature, sun illumination and other environmental forcings (wind speed, sea tides and thermoaline currents).

In particular, during AREX 2006, large plankton blooms were monitored in their initial stage of development in the northern and central west Spitsbergen marine area, while in the successive campaign this scenario reappeared in the southern region.

Strong correlations among different dissolved and particulate seawater matters have been observed and discussed. The operation of CASPER allowed the simultaneous measurement of seven classes of fluorescing components: in particular, the very small NADPH and carotenoids fluorescence has been detected.

The large database of fluorescence spectra showed the advantage of being a suitable input for a refined and complete statistical analysis, that supplied robust information on the different waters monitored during the oceanographic campaigns.

The dataset collected during AREX 2006 and 2007 can be used for ocean color satellite radiometer calibration/validation activities. In particular, it can be helpful to develop a regional bio-optical algorithm for the Arctic Ocean.

Acknowledgements

We gratefully acknowledge the valuable support by Polish researchers not included in the author list and by the crew of the R/V Oceania. CASPER and ELF have been developed with the support of MIUR (Italian Ministry of Education, University and Research), in the framework of the projects RIADE (integrated research for applying new technologies and processes for combating desertification) and MIAO (microsystems for hostile environments), respectively. E. Demetrio and I.G. Okladnikov acknowledge support by FILAS (Finance Company for the Development of Latium) and ENEA (Italian National Agency for New Technologies, Energy and the Environment) fellowships, respectively.

References

[1] K. Aagaard, A. Foldvik, S. R. Hillman, Journal of Geophysical Research **92**, 3778-3784 (1987).

[2] R. Barbini, F. Colao, R. Fantoni, A. Palucci, S. Ribezzo, The ENEA fluorosensor system used in monitoring the Adriatic Sea. In: Remote Sensing of Vegetation and Sea, G. Cecchi, G. D'Urso, E. T. Engman, P. Gudmansen, Eds. SPIE Proceedings, Vol. **2959**, 254-264 (1996a).

[3] R. Barbini, F. Colao, R. Fantoni, A. Palucci, S. Ribezzo, C. Micheli, Lidar Fluorosensor System for Remote Monitoring Phytoplankton Blooms in the Swedish Marine Campaign. ENEA Report RT/INN/96/24 (1996b).

[4] R. Barbini, R. Fantoni, F. Colao, A. Palucci, S. Ribezzo, International Journal of Remote Sensing **20**, 2405-2421 (1999).

[5] R. Barbini, F. Colao, R. Fantoni, G. M. Ferrari, A. Lai, A. Palucci, International Journal of Remote Sensing **24**, 3191-3204 (2003).

[6] R. Barbini, F. Colao, R. Fantoni, A. Palucci, S. Ribezzo, J. Remote Sensing, **22**(2 & 3), 369–384 (2001).

[7] D. Caputo-Rapti, L. Fiorani, A. Palucci, J. Optoelectron. Adv. Mater. **10**(2), 461 – 469 (2008).

[8] Climate Change 2007: Synthesis Report. Summary for Policymakers. http://www.ipcc.ch/pdf/assessment-report/ar4/syr/ar4_syr_spm.pdf

[9] C. D. Clark, W. T. Hiscock, F. J. Millero, G. Hitchcock, L. Brand, W. L. Miller, L. Ziolkowski, R. F. Chen, R. G. Ziza, CDOM distribution and CO2 production on the Southwest Florida Shelf. Marine Chemistry **89**, 145-167 (2004).
[10] F. Colao, R. Fantoni, L. Fiorani, V. Lazic, A. Palucci, E. Demetrio, I. Okladnikov, Technical Reports of the Italian Agency for New Technologies, Energy and the Environment, Rome, Italy, RT/2007/43/FIM (2008).
[11] P. G. Coble, S. A. Green, N. V. Blough, R. B. Gagosian, Nature, **348**, 432-434 (1990).
[12] S. Determann, J. M. Lobbes, R. Reuter, J. Rullkotterb, Marine Chemistry **62**, 137–156 (1998).
[13] L. Fiorani, I. G. Okladnikov, A. Palucci, J. Optoelectron. Adv. Mater. **10**(6), 1482 – 1488 (2008).
[14] H. Hop, T. Pearson, E. N. Hegseth, K. M. Kovacs, C. Wiencke, S. Kwasniewski, K. Eiane, F. Mehlum, B. Gulliksen, M. Wlodarska-Kowalezuk, C. Lydersen, J. M. Weslawski, S. Cochrane, G. W. Gabrielsen, R. J. G. Leakey, O. J. Lonne, M. Zajaczkowski, S. Falk-Petersen, M. Kendall, S. A. Wangberg, K. Bischof, A. Y. Voronkov, N. A. Kovaltchouk, J. Wiktor, M. Poltermann, G. di Prisco, C. Papucci, S. Gerland, Polar Research **21**(1), 167-208 (2002).
[15] Inall, M. & Parker, P. 1992: Sea ice. In E. Rachor (ed): Scientific Cruise Report of the 1991 Arctic Expedition ARK VIIID of RV POLARSTERN (EPOS II: Study of the European Arctic SheK "SEAS", of the European Science Foundation). Ber. Polarjiorscli. **115**, 43-5 1.
[16] I. T. Jolliffe, Principal Component Analysis, Springer, New York, US, 2002.
[17] W. Maslowski. Advanced Modeling of the Arctic Ocean and Sea Ice in Support of Global Climate Studies, Proceedings of the Global Change Workshop on Polar Processes, Ed. D. Martinson, Amer. Meteorol. Soc., pp. 93-96, (1996).
[18] K. A. Orvik, P. Niiler, Geophys. Res. Lett. **29**(19), 1896, doi:10.1029/2002GL015002 (2002).
[19] G. Owrid, G. Socal, G. Civitarese, A. Luchetta, J. Wiktor, E.-M. Nöthig, I. Andressen, U. Schauer, V. Strass, Polar Research **19**(2), 155-171.
[20] A. Palucci, Optics of Biological Particles, A. Hoekstra, V. Maltsev, G. Videen, Eds. NATO Science Series, **238**, 165-192 (2006).
[21] J. Piechura, W. Walczowski The Arctic Front: Structure and dynamics, Oceanologia, **37**(1), 47– 73 (1995).
[22] J. Piechura, A. Beszcynska-Moller, R. Osinski, 2001: Volume, heat and salt transport by the West Spitsbergen Current. Polar Research, **20**, 233-240.
[23] P. Schlichtholz, M.-N. Houssais, Deep-Sea Research II **46**, 1137-1168 (1999).
[24] A. P. Shreve, J. K. Trautman, T. G. Owens, A. C. Albrecht, Chemistry Physics, **154**, 171-178 (1991).
[25] S. Steigenberger, F. Terjung, H .P. Grossart, R. Reuter, Blue-Fluorescence Of Nadph As An Indicator of Marine Primary Production EARSeL eProceedings 3, 1/2004 18.
[26] W. Walczowski, J. Piechura, Geophysical Research Letters **34**, L10608 (5 pp.) (2007).
[27] www.iopan.gda.pl
[28] www.damocles-eu.org
[29] www.riade.net

*Corresponding author: antonio.palucci@enea.it